Vibration control of structures with interferometric sensor non-linearity

2004 Smart Mater. Struct. 13 92

(http://iopscience.iop.org/0964-1726/13/1/011)

INSTITUTE OF PHYSICS PUBLISHING SMART MATERIALS AND STRUCTURES
Smart Mater. Struct. **13** (2004) 92–99 PII: S0964-1726(04)71619-5

Vibration control of structures with interferometric sensor non-linearity

Do-Hyung Kim, Jae-Hung Han, Dae-Hyun Kim and In Lee[1]

Department of Aerospace Engineering, Korea Advanced Institute of Science and Technology, 373-1 Guseong-dong, Yuseong-gu, Daejeon 305-701, Korea

E-mail: inlee@asdl.kaist.ac.kr

Received 7 March 2003, in final form 31 October 2003
Published 15 December 2003
Online at stacks.iop.org/SMS/13/92 (DOI: 10.1088/0964-1726/13/1/011)

Abstract
Experimental studies on vibration control of a composite beam with a piezoelectric actuator and an extrinsic Fabry–Perot interferometer (EFPI) have been performed using a neural network controller. Because of their interferometric characteristics, EFPI sensors show non-linearity as dynamic amplitude increases. Within the linear range of EFPI, conventional control algorithms can be applied without serious difficulty. However, closed-loop control may make the target system unstable when sensor non-linearity gets high. Therefore, we examine the effects of the non-linearity of the sensor on the control stability and performance, and investigate any simple method applicable to the vibrations beyond the linear range. For this purpose, a neural controller is adopted and its performance is experimentally investigated. The neuro-controller showed good performance and adaptiveness to the sensor's non-linearity. Although the present neuro-controller is not a fundamental solution to vibration control of structural systems, it can be a simple practical choice for systems with sensor non-linearity.

1. Introduction

There has been increasing interest in vibration control of structural systems using smart materials [1, 2]. In order to realize this function of smart structures, many researchers have studied functional materials, their characteristics, and the analysis methods of smart structures. They have also investigated sensor and actuator placement problem, controller designs, and many other relevant research topics. Among several functional materials, optical fibers are the preferred sensor materials; they can produce sensors that are small, lightweight, less power consuming, immune to electromagnetic interference, and easily installable onto/into host structures. In addition, the optical interferometer sensor is one of the most effective strain sensors in terms of resolution. Since the optical fibers can be inserted in the laminated composite structure, they can directly measure internal strain states inside the structure as well as surface strain, unlike conventional strain sensors. Optical fiber sensors have been utilized in dynamic measurement and vibration control as well as health monitoring. Yang and Jeng [3] showed that bending vibration could be effectively reduced by using the optical fiber as a Michelson interferometer for the detection of the structural vibration and the lead–zirconium–titanate (PZT) actuator. Chun *et al* [4] performed the direct negative velocity feedback control of a carbon/epoxy laminated beam using a Fabry–Perot interferometer and a piezoceramic actuator.

Among various kinds of optical fiber sensors, interferometric sensors are widely used because they have a lot of the advantages of other optical sensors and can be constructed at reasonable prices. However, it is reported that they have a problem representing vibrational amplitudes and directions because of their interferometric characteristics. In order to extract true mechanical strain from the EFPI sensor output signal, several methods have been proposed including quadrature phase-shifted EFPI [5], absolute EFPI [6], and passive quadratic signal processing using two read-out interferometers [7]. Several signal processing techniques have also been used based on fringe counting methods [8, 9]. Such algorithms can be applicable for the strain measurement of quasi-static systems, but are not practical for real-time feedback control

[1] Author to whom any correspondence should be addressed.

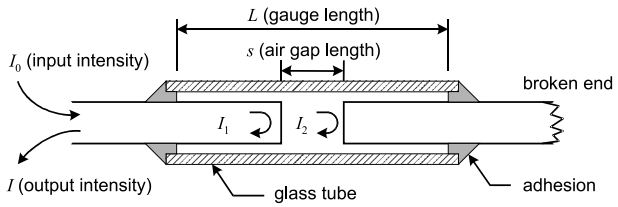

Figure 1. Schematic diagram of an EFPI.

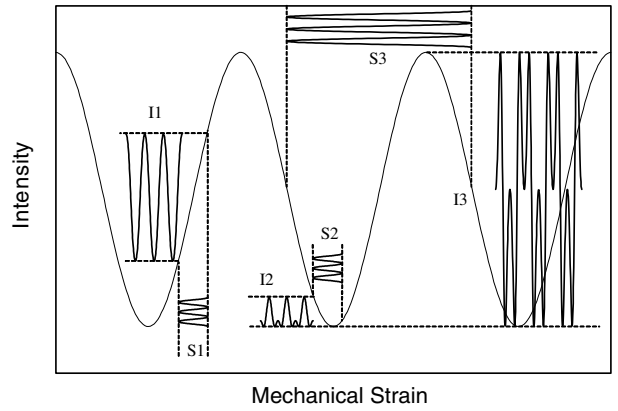

Figure 2. Relationship between sensor output intensities and strain variations.

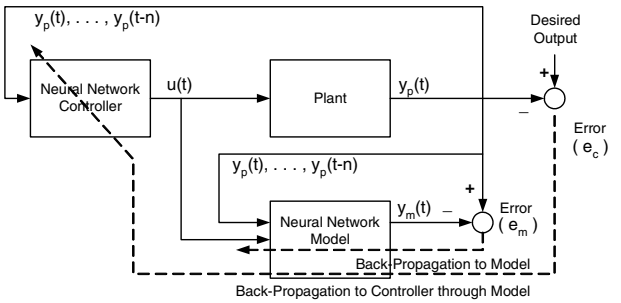

Figure 3. Overall architecture for the neuro-controller with the neural network model.

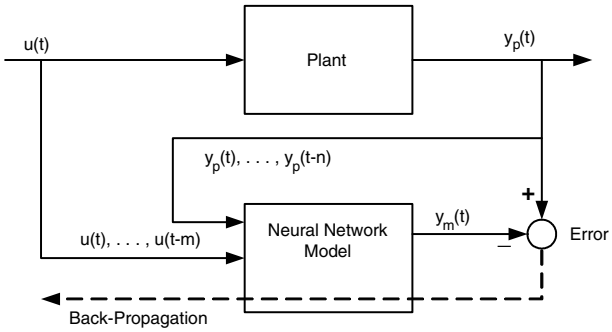

Figure 4. Forward modeling using the neural network.

systems. That is the why studies on vibration control using interferometric optical sensors are limited to small disturbance cases [3, 4].

If a dynamic system has non-linear characteristics, such as interferometric sensors used for large dynamic strain measurement, a linear controller may make the system unstable. Control systems can be subdivided into two categories: highly specialized controllers and general purpose controllers. Highly specialized controllers are relevant when the system to be controlled is in some sense difficult to stabilize or when the performance is extremely important. The use of general purpose controllers means that the same controller structure can be used on a wide class of practical systems, and the controllers are characterized by being simple to tune so that satisfactory performance can be achieved with modest effort [10]. Basically, neural networks belong to the latter, and their ability to model a wide class of systems in many applications can reduce time spent on development and offer a better performance than can be obtained with a conventional technique. At the same time, neural networks can be regarded as highly specialized controllers because of their successful application to many non-linear and very specific applications. The research on neural network based vibration controls can be divided into two categories: feedforward and feedback control methods. Feedforward controls generally utilize a reference signal, which is correlated with the impending primary disturbance, for the derivation of control input. Snyder and Tanaka [11] developed a neural network/algorithm, which can be regarded as a non-linear generalization of the transversal filter/filtered-x least mean squares (LMS) algorithm, for non-linear feedforward control systems. They conducted experimental works to demonstrate the utility of the algorithm, showing that it is well suited for a non-linear control problem. On the other hand, feedback controls generally rely on the error signals to construct control signals for the non-availability of the reference signals. Chandrashekhara and Smyser [12] developed a numerical dynamic model for the active vibration control of laminated doubly curved shells. In their study, a neural network controller was designed and trained off-line to emulate the performance of a linear quadratic Gaussian with loop transfer recovery (LQG/LTR) controller. Vibration controls using neural networks with optimal neural design methodologies using the Taguchi method have also been studied [13]. Youn *et al* [14] applied a neuro-adaptive feedback control algorithm to suppress the vibrations of composite structures subject to sudden delamination. They used several composite beams with a delaminated piezoelectric actuator as experimental models in order to realize sudden delamination conditions.

The present paper experimentally investigates vibration control performance when the EFPI sensor produces a non-linear signal. We examine the effects of non-linearity of the sensor on the control stability and performance, and investigate any simple method applicable to the vibrations beyond the linear range. For this purpose, a neural controller is adopted and its performance is experimentally investigated.

2. Extrinsic Fabry–Perot interferometer sensor

In this study, an EFPI is fabricated and used as a sensor in vibration control system. Its schematic diagram is shown in figure 1. The reflected intensity, I, can be written as a sinusoidal function as follows [15]:

$$I \propto A + B\cos\phi \tag{1}$$

where A and B are functions of the fiber core radius, the air gap separation, the transmission coefficient of the air/glass

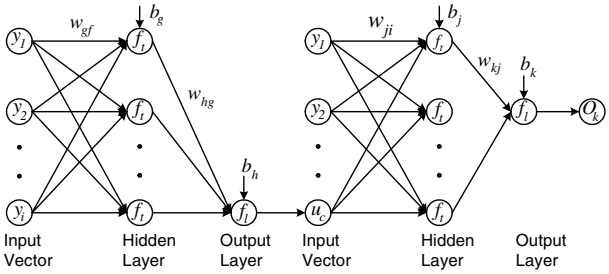

Figure 5. Connection of the neural network model and neuro-controller.

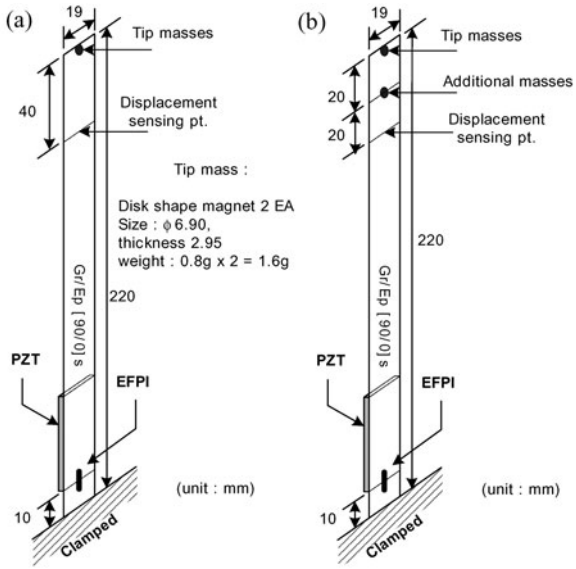

Figure 6. Schematic diagram of the specimens. (a) Nominal system. (b) Modified system.

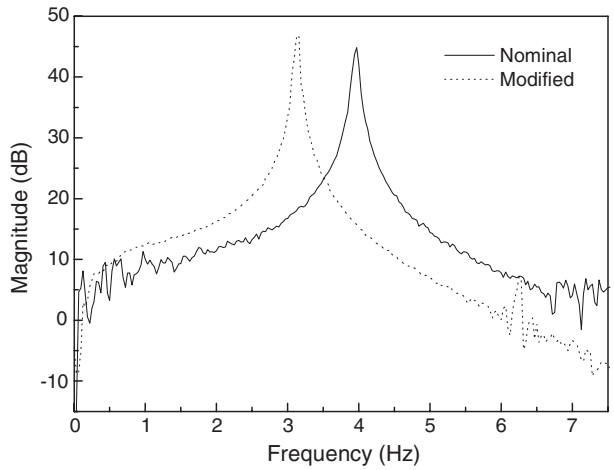

Figure 7. Frequency response functions of the nominal and modified systems.

interface, and the numerical aperture, and ϕ is the optical phase. For small variations of air gap separation, variations of A and B are negligible. The relation between the optical phase, ϕ, and the gap separation, s, is given as

$$\phi = 2ks \tag{2}$$

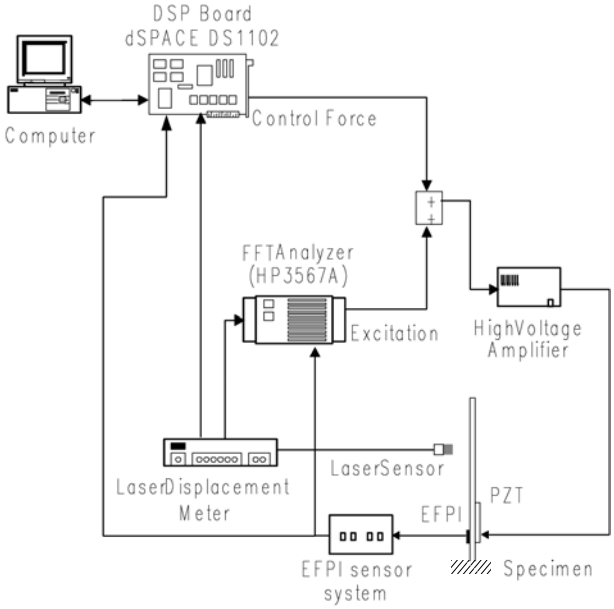

Figure 8. Experimental setup for the vibration control.

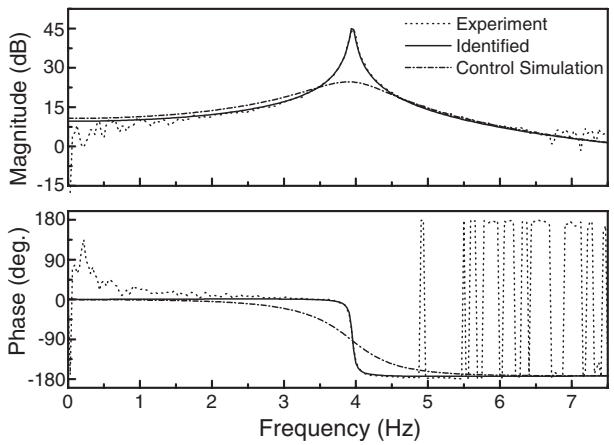

Figure 9. System identification and simulated frequency responses.

where k is the wavenumber defined as $2\pi n_c/\lambda_0$, n_c is the refractive index of the EFPI in the gauge length, and λ_0 is the wavelength of the laser diode in the vacuum state (1310 nm, in this study). Using equation (2) and the definition of k, $\Delta\phi$ can be written as follows:

$$\Delta\phi = \frac{4\pi}{\lambda_0}(n_c\Delta s + \Delta n_c s) = \frac{4\pi}{\lambda_0}(n_c\Delta L + \Delta n_c s). \tag{3}$$

There is no change of refractive index in the gauge length since the light medium of EFPI is air, so $n_c \cong 1$ and $\Delta n_c \cong 0$. Since Δn_c is almost zero, EFPIs have immunity to polarization fading and transverse strain intensity. Using $n_c \cong 1$, $\Delta n_c \cong 0$, and $\lambda_0 = 1310$ nm, $\Delta\phi$ is reduced to

$$\Delta\phi = 0.9593 \times 10^7 \Delta L \text{ (rad m}^{-1}\text{)}. \tag{4}$$

In order to fabricate an EFPI as shown in figure 1, the ends of a pure silica capillary tube were bonded to the optical fibers with epoxy. The Fresnel reflection, I_1, from the glass/air interface at front of air gap, s, and the reflection, I_2, from

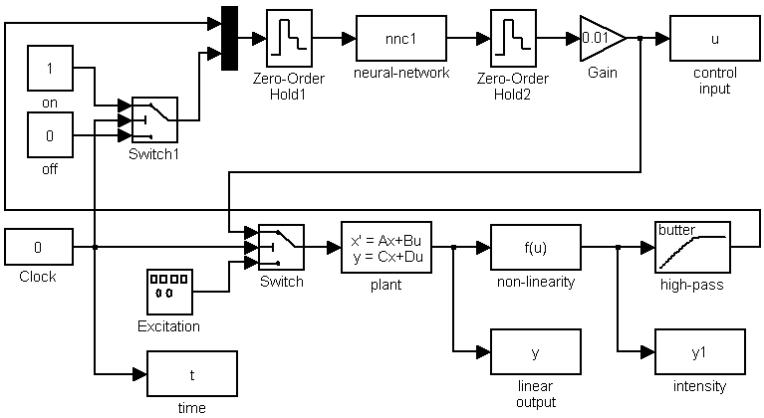

Figure 10. Block diagram for vibration control simulation.

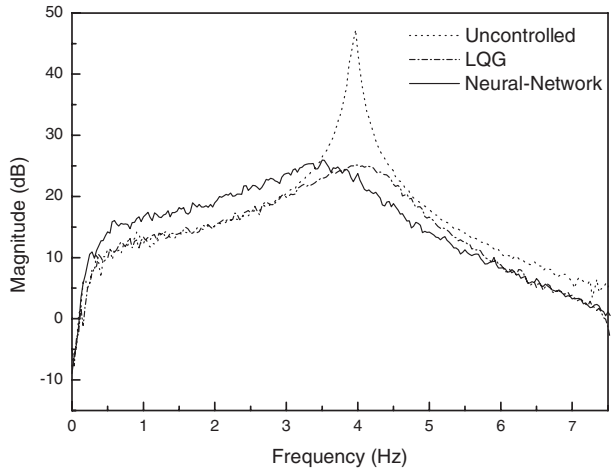

Figure 11. Responses to random excitation (nominal system).

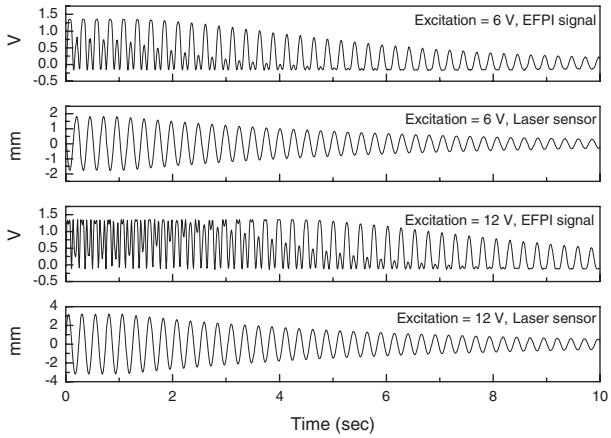

Figure 12. Free decay signals for excitation voltage = 6 and 12 V (nominal system).

the air/glass interface at the far end of air gap interfere in the input/output fiber. The measured gauge length, L, and the air gap separation, s, were about 5.1 mm and 15 μm, respectively.

Because of the characteristics of interferometric optical fiber sensors, the output intensity of an EFPI does not have a linear relationship with mechanical strain, as shown in figure 2. S1 is a possible mechanical strain for a vibrating system and I1 is the corresponding output intensity. S2 indicates another example of mechanical strain that has the same amplitude as S1. However, the corresponding intensity, I2, shows a distorted behavior, according to the initial optical phase of EFPI. You can easily see from S3 and I3 that the EFPI sensor shows non-linearity whenever the strain amplitude is large enough. As previously stated, the reconstruction of mechanical strain from an EFPI sensor signal cannot be easily applied to real-time vibration control. Therefore, it can be a simple practical choice to use the raw EFPI sensor signal for vibration control. In that case, it is necessary to consider the non-linear characteristics of an EFPI sensor. For a dynamic system with sensor non-linearity, a conventional linear controller may have performance and stability problems. Therefore, a neural network controller is adopted to deal with vibration control problems for systems containing sensors with non-linearity.

3. Neural network controller

A neural network is a mathematical model, which is artificially embodied by imitating the recognition or knowledge-acquiring processes of human beings. A neural network consists of neurons, weights, and biases. Learning is defined as a process that tunes weights and biases so as to obtain the desired output values of the neural network.

The overall structure and learning algorithm of the neural network are similar to those of [13]. The neural network used in this study consists of one input vector and two layers, one hidden layer and one output layer. A tangent sigmoid activation function was used for the hidden layer and a linear activation function was used for the output layer. For simplification, bias was not used in the network. Among several learning algorithms, the error back-propagation learning rule was used and the momentum method was applied in order to improve convergence characteristics and the convergence speed. The fundamental idea of the algorithm is to adjust weights and biases of neural network so that the sum of squared error of the outputs is minimized. Using a gradient descent procedure, weights are updated in real-time.

The control system consists of the neuro-identification model and the neuro-controller, and the overall architecture of the controller is shown in figure 3. The role of the

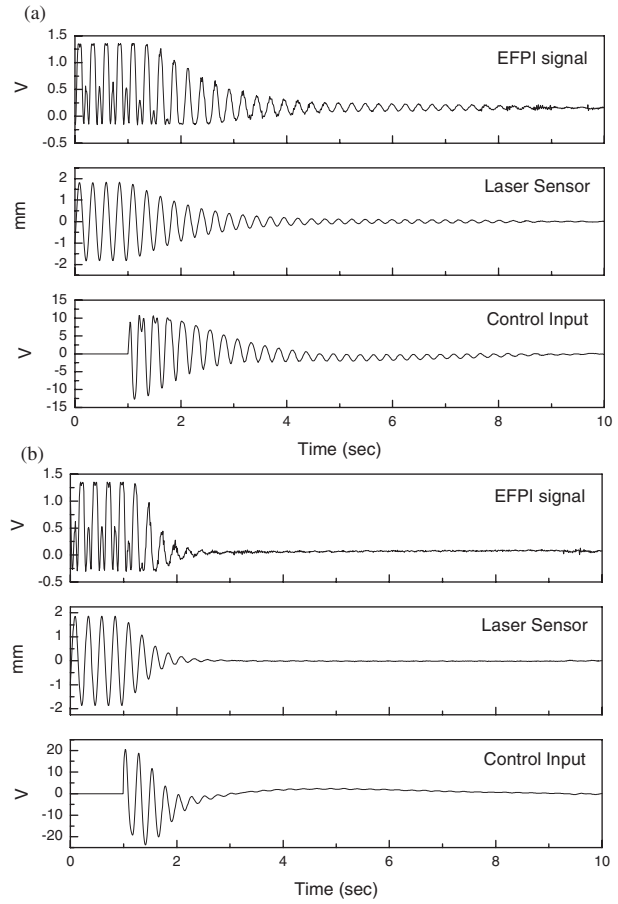

Figure 13. Control result of the nominal system (excitation voltage = 6 V). (a) Neuro-controller. (b) LQG controller.

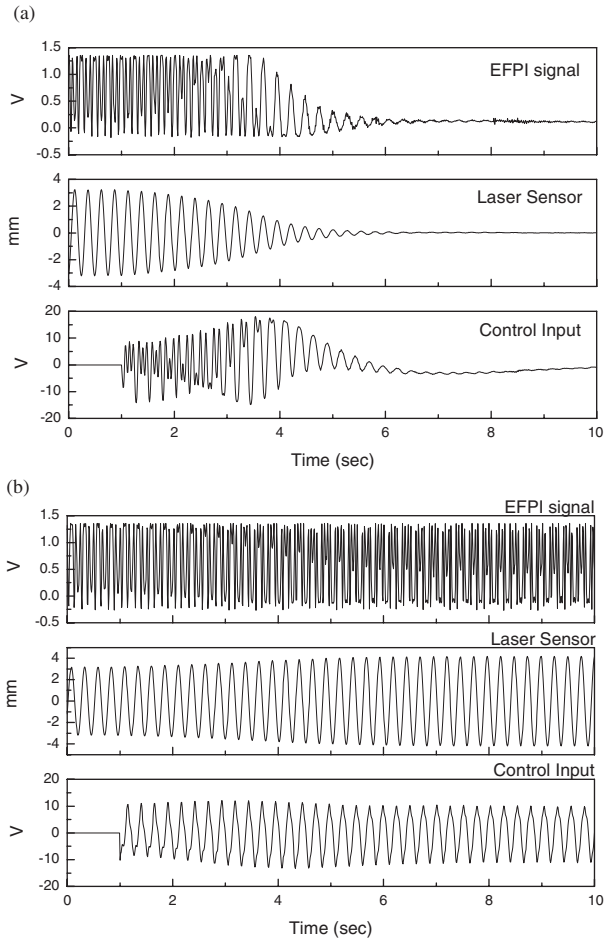

Figure 14. Control result of the nominal system (excitation voltage = 12 V). (a) Neuro-controller. (b) LQG controller.

neural network model (identifier) for the plant is to obtain mathematical representation of the real plant. This procedure is called forward modeling. The neural network model is located in parallel with the plant as shown in figure 4. The weights of the neural network model are adjusted to make the output of the neural network model the same as that of the plant. The input vector of the neural network model consists of the present and previous plant inputs and outputs. In other words, the output value of neural network model y_m is calculated by using time sequences of the plant input u and plant output y_p as follows:

$$y_m(t+1) = f(y_p(t), \ldots, y_p(t-n); u(t), \ldots, u(t-m)). \quad (5)$$

After completing the forward modeling, the tuning for weights of the neuro-controller is performed by the error back-propagation learning algorithm. Because the desired output value of the neuro-controller is not given in advance, this value should be calculated by the error back-propagation through the neural network plant model, as shown in figure 5. In this step, the desired output value of the plant is set to zero because the purpose of the control is to suppress vibrations. When adjusting the weights of the neuro-controller, those of the neural network model are not changed. The output of the neuro-controller, u_c, is calculated by using time sequences of the plant output, y_p, as follows:

$$u_c(t) = f(y_p(t-1), y_p(t-2), \ldots, y_p(t-n)). \quad (6)$$

The neuro-controller has five input values, and eight neurons and one neuron for the hidden and output layers, respectively. The output value of the neuro-controller is used as both the control force of the plant and the fifth input of neural network model. Here, the control force is the applied voltage to the piezoceramic actuator. The five previous output values of the plant are used as input of the neuro-controller. The neural network model has the same structure as neuro-controller. The four previous output values of the plant and the output of the neuro-controller are used as the input values of the neural network model.

4. Experimental results and discussion

The schematic diagram of the specimen is shown in figure 6. The nominal system comprises a composite base structure (graphite/epoxy $[90/0]_s$), a PZT actuator (C8, Fuji Ceramics), an EFPI sensor, and tip masses for the reduction of resonant frequencies. In the experiment, the EFPI output is used as the feedback signal and a laser displacement sensor (LB041, Keyence) is used for the monitoring of real deflections. In many practical situations, the system dynamics may change during operation. Therefore, a controller is required to exhibit robustness with respect to the system variations. To investigate the adaptiveness of the controller, a modified system is

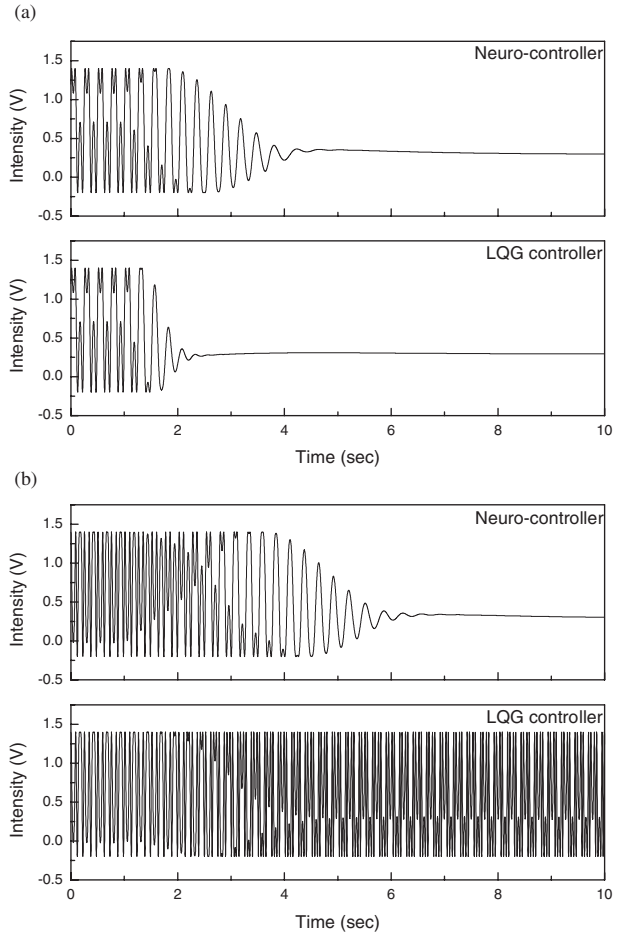

Figure 15. Simulation result for an example system. (a) Small amplitude case. (b) Large amplitude case.

prepared. The modified system has a reduced resonant frequency compared with the nominal system (3.97 Hz → 3.16 Hz). Figure 7 shows the variation of the frequency response functions due to additional tip masses.

The overall experimental setup for the vibration control is shown in figure 8. The excitation signal and control input are amplified through the high voltage amplifier (HEOPS-5B6, Matsusada) and fed into the piezoceramic actuator. The designed neural network controller is implemented using a DSP board (DS1102, dSPACE) and the weights are updated every 0.01 s. In the random excitation experiment, an HP3567A spectrum analyzer is used to obtain frequency response functions.

An LQG controller is also designed and the control performance examined. In the case of the neural network control, a mathematical model is constructed during a real-time learning procedure. However, an LQG controller is a model based controller. The design of the LQG controller is based on the identified system model using the experimental frequency response function of the nominal system. The noise matrix, Θ, for the measurement noise, $\theta(t)$, is calculated from the sensor output when the specimen is stationary. For the process noise, the covariance is assumed to be the same as the measurement noise. The weighting matrix $\mathbf{R}$ is fixed to identity, $\mathbf{R} = [1]$, and $\mathbf{Q}$ is considered to be diagonal. The simulated frequency response of the closed-loop system using the designed LQG

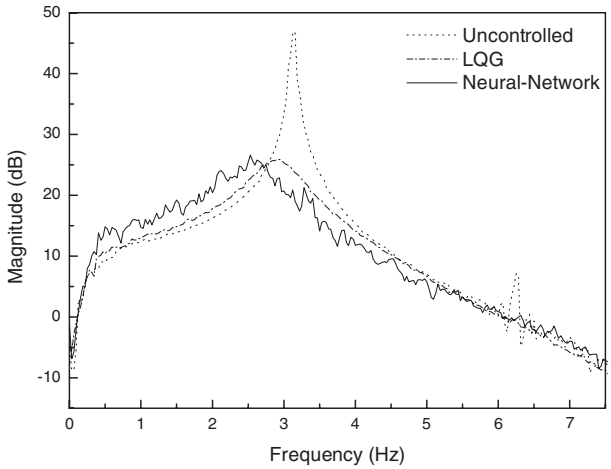

Figure 16. Responses to random excitation (modified system).

controller is shown in figure 9, and the designed LQG controller in cascade realization is as follows [16]:

$$F(s) := \left[\begin{array}{c|c} \mathbf{A} - \mathbf{B}\mathbf{K_c} - \mathbf{K_f}\mathbf{C} & \mathbf{K_f} \\ \hline \mathbf{K_c} & \mathbf{0} \end{array}\right] = \left[\begin{array}{c|c} \mathbf{a_f} & \mathbf{b_f} \\ \hline \mathbf{c_f} & \mathbf{d_f} \end{array}\right]$$

($F(s)$: the transfer function from $\mathbf{y}$ to $-\mathbf{u}$)

$$\mathbf{a_f} = \begin{bmatrix} -11.015 & 20.716 \\ -29.276 & -9.6763 \end{bmatrix}, \qquad \mathbf{b_f} = \begin{bmatrix} -1.1004 \\ -0.831\,41 \end{bmatrix}$$

$$\mathbf{c_f} = [\,0.414\,19 \quad -0.707\,00\,], \qquad \mathbf{d_f} = [0]. \tag{7}$$

Vibration control experiments have been performed in the frequency and the time domains. For the frequency domain experiment, band-limited white noise has been used as the excitation signal. The random excitation was small enough that the EFPI sensor output signal was within the linear range. A sinusoidal excitation signal was applied for the time domain experiments. Both slightly and highly non-linear cases have been considered in the time domain experiments. In addition to experiments, vibration control simulation has been performed. In this case, an example dynamic system is introduced which is constructed as a combination of the identified linear system model and a non-linear sensor output part. Interferometric sensor output is assumed to be in the form of equation (1) as follows:

$$I = A + B\cos(y + \phi_0)$$
$$A = 0.6, \qquad B = 0.8, \qquad \phi_0 = 5\pi/8 \tag{8}$$

where y is the output of the linear system model. Matlab/Simulink is used for the simulation and the block diagram is shown in figure 10. The plant model is the same model as used in the LQG controller design, and the parameters in equation (8) are chosen to represent similar output intensity to the experimental result for nominal case.

4.1. Experimental result for the nominal system

For the nominal system, experimental frequency response functions of the uncontrolled and controlled systems are shown in figure 11. EFPI sensor output is approximately linear for small disturbances. Hence, both the neuro-controller and the

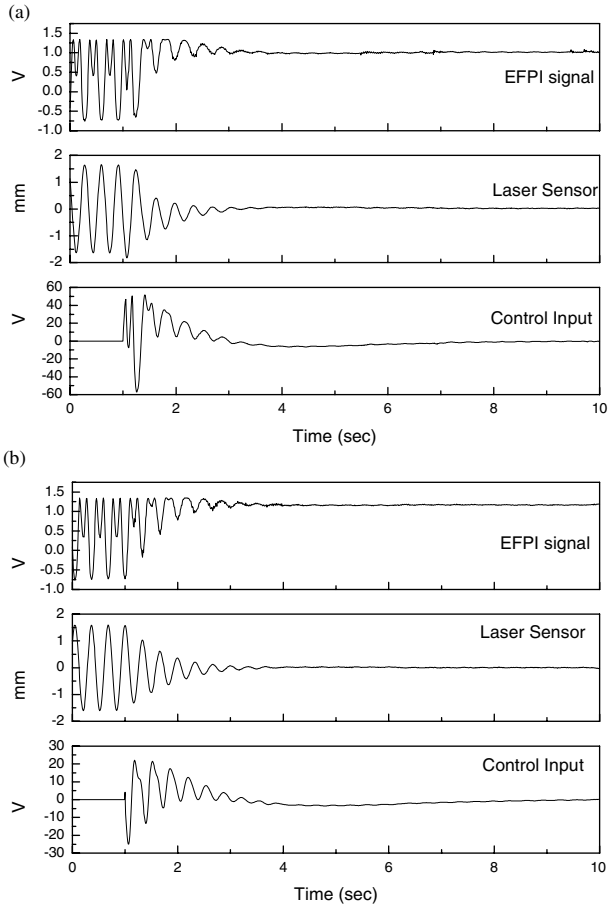

Figure 17. Control result of the modified system (excitation voltage = 6 V). (a) Neuro-controller. (b) LQG controller.

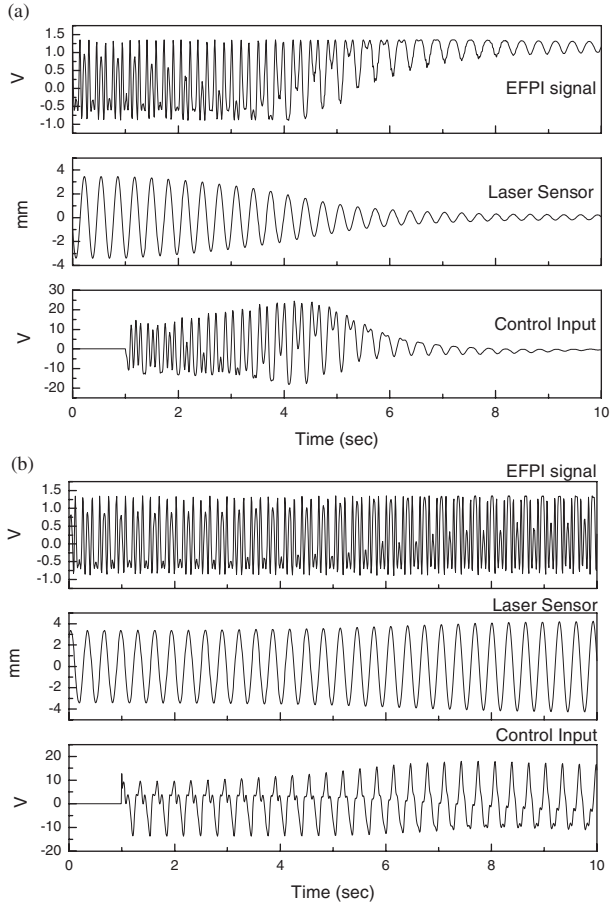

Figure 18. Control result of the modified system (excitation voltage = 13 V). (a) Neuro-controller. (b) LQG controller.

LQG controller show good performance. Figure 12 shows the free decay signals when an excitation signal with resonant frequency is supplied to the piezoceramic actuator until the specimen vibrates in a steady state and then the excitation is stopped at 1 s. It is seen that the EFPI sensor output signal becomes more distorted as the vibration amplitude increases. Vibration control experiments have been performed for small and large amplitude cases, that is, for slightly and highly non-linear cases. Figures 13 and 14 show the control results when an excitation signal with the open-loop resonant frequency is supplied until the specimen vibrates in a steady state and then the excitation is removed and a control force is applied simultaneously at 1 s. When the excitation amplitude is small, the EFPI signal is slightly distorted and both controllers can suppress the vibration successfully. However, the LQG controller makes the system unstable as the excitation amplitude is increased. The EFPI sensor's interferometric non-linearity can cause a serious problem in vibration control. The neuro-controller showed good performance and adaptiveness to the sensor's non-linearity. However, it also fails in vibration suppression when the sensor signal gets excessively non-linear. We get a similar simulation result, as shown in figure 15. It has the same excitation and control start condition as the experiment.

4.2. Experimental results for the modified system

The same procedure and controllers are applied to the modified system. For random excitation, there is no noticeable degradation of control performance because the variation of the resonant frequency is not very large, as shown in figure 16. The control results for the sinusoidal excitation are also similar to those of the nominal system, as shown in figures 17 and 18. As the excitation amplitude is increased, the EFPI sensor shows more non-linear behavior and the controllers operate less efficiently when the vibration amplitude is over a certain level.

5. Conclusion

In the present study, the effects of a sensor's non-linearity on the feedback control system have been examined. A neural network based adaptive control was applied to the vibration control of a structural system with the sensor's non-linearity, and an LQG controller was also designed and applied to the vibration control. It is found that a small amount of non-linearity does not cause a problem in the feedback loop. However, a controller may make the target system unstable when the sensor non-linearity gets high. This paper begins research into overcoming interferometric non-linearity in structural vibration control by using one of the general purpose controllers, namely neural networks. With minimum

tuning of the control parameters, the neuro-controller showed good performance and adaptiveness to the sensor's non-linearity. Although the present neuro-controller is not a fundamental solution to vibration control of structural systems, it can be a simple practical choice for systems with sensor non-linearity. In order to apply EFPI sensors to vibration control over a much wider dynamic range, a real-time linearization technique is now under investigation by the present authors.

Acknowledgment

The present study has been supported by a grant from the National Research Laboratory Program of the Ministry of Science and Technology, Korea. The authors gratefully acknowledge this support (Subject No. 2000-N-NL-01-C-250).

References

[1] Bailey T and Hubbard J E Jr 1985 Distributed piezoelectric polymer active vibration control of a cantilever beam *J. Guid. Control Dyn.* **8** 605–11

[2] Han J-H, Rew K-H and Lee I 1997 An experimental study for active vibration control of composite structures with a piezo-ceramic actuator and a piezo-film sensor *Smart Mater. Struct.* **6** 549–58

[3] Yang S M and Jeng J A 1997 Vibration control of a composite plate with embedded optical fiber sensor and piezoelecric actuator *J. Intell. Mater. Syst. Struct.* **8** 393–400

[4] Chun B-S, Park W-S, Park H-C, Hwang W and Han K-S 1997 Vibration control of laminated composite beam using optical fiber sensor *Proc. 5th Japan Int. SAMPE Symp.* (Tokyo: SAMPE) pp 961–6

[5] Murphy K A, Gunther M F, Vengsarkar A M and Claus R O 1991 Quadrature phase-shifted, extrinsic Fabry–Perot optical fiber sensors *Opt. Lett.* **16** 273–5

[6] Tran T A, Greene J A, Murphy K A and Bhatia V 1995 EFPI manufacturing improvements for enhanced performance and reliability *Proc. SPIE* **2247** 312–23

[7] Lo Y L and Sirkis J S 1997 Passive signal processing of in-line fiber etalon sensors for high strain-rate loading *J. Lightwave Technol.* **15** 1578–86

[8] Kim S H, Lee J J and Kwon D S 2001 Signal processing algorithm for transmission-type Fabry–Perot interferometric optical fiber sensor *Smart Mater. Struct.* **10** 736–42

[9] Kwon I B, Kim C G and Hong C S 1999 A digital signal processing algorithm for structural strain measurement by 3×3 passive demodulated fiber optic interferometric sensor *Smart Mater. Struct.* **8** 433–40

[10] Norgaard M, Ravn O, Poulsen N K and Hansen L K 2000 *Neural Networks for Modelling and Control of Dynamic Systems* (Great Britain: Springer)

[11] Snyder S D and Tanaka N 1995 Active control of vibration using a neural network *IEEE Trans. Neural Netw.* **6** 819–28

[12] Chandrashekhara K and Smyser C P 1998 Dynamic modeling and neural control of composite shells using piezoelectric devices *J. Intell. Mater. Syst. Struct.* **9** 29–43

[13] Yang S M and Lee G S 1998 An optimal neural network design methodology for fast convergence and vibration suppression *J. Intell. Mater. Syst. Struct.* **9** 999–1008

[14] Youn S-H, Han J-H and Lee I 2000 Neuro-adaptive vibration control of composite beams subject to sudden delamination *J. Sound Vib.* **238** 215–31

[15] Park J-W, Ryu C-Y, Kang H-K and Hong C-S 2000 Detection of buckling and crack growth in the delaminated composites using fiber optic sensor *J. Compos. Mater.* **34** 1602–23

[16] Dorato P, Abdallah C and Cerone V 1995 *Linear Quadratic Control* (Englewood Cliffs, NJ: Prentice-Hall) pp 99–118